Available online at www.sciencedirect.com
SCIENCE DIRECT
Dyes and Pigments 73 (2007) 224–229
DYES and PIGMENTS
www.elsevier.com/locate/dyepig

Spirosilabifluorene linked bistriphenylamine: Synthesis and application in hole transporting and two-photon fluorescent imaging

Haibo Xiao, Han Shen, Yougang Lin, Jianhua Su, He Tian*

Laboratory for Advanced Materials and Institute of Fine Chemicals, East China University of Science and Technology, Shanghai 200237, PR China

Received 15 July 2005; received in revised form 11 October 2005; accepted 23 November 2005
Available online 19 January 2006

Abstract

Spirosila-BF-TPA, in which two identical triphenylamines linked orthogonally around a spirosilabifluorene core, has been synthesized and characterized. The introduction of a spiro linkage into the structure of spirosila-BF-TPA leads to a reduction in crystallization tendency and no glass transition temperature was observed. Spirosila-BF-TPA exhibits blue emission around 410 nm. Its reversible electrochemical oxidation and low ionization potential (5.33 eV) suggest that spirosila-BF-TPA might have potential application as a hole transporting material. The hole transport ability of spirosila-BF-TPA was tested by comparing the performance of the two types of OLED devices. According to the fluorescence images of spirosila-BF-TPA films, it was found that the two-photon fluorescence of spirosila-BF-TPA is intensive, which implies that this molecule is also a promising candidate for an application such as two-photon microscopy and imaging.

Keywords: Spirosilabifluorene linked bistriphenylamine; Hole transporting; Two-photon fluorescent imaging

1. Introduction

Triarylamines have attracted considerable interest as hole transport materials for use in multilayer organic electroluminescence (EL) devices due to their relatively high mobilities and their low ionization potentials [1–5]. However, triphenylamine (TPA) has the tendency to crystallize upon exposure to heat and is rarely used for electroluminescent device applications. A considerable amount of evidence indicates that an amorphous thin film (in OLEDs) with a high glass transition temperature (T_g) is less vulnerable to heat and, hence, the device performance is more stable [6–10]. Salbeck et al. introduced the concept of linking two arylamine moieties via a spiro carbon center, introducing a 90° angle between them [11–13]. This structural feature not only hinders close packing and intermolecular interactions, but also increases the molecular rigidity. As a result, the introduction of a spirobifluorene linkage into the structure of small molecules leads to a reduction in the tendency to crystallize, an enhancement in solubility, and an increase in glass transition temperature. The melting point of 9,9′-spirobifluorene is 198 °C, while 9,9′-spiro-9-silabifluorine (SSBF) is 227 °C. Compared to the compounds containing 9,9′-spirobifluorene, the compounds containing 9,9′-spiro-9-silabifluorene may have an improved morphological stability in films [14–16].

Organic two-photon induced fluorescent (TPIF) materials have been widely studied recently due to their various applications, especially in TPIF microscopy [17–19]. However, the study of TPIF molecules with efficient two-photon induced blue emission is still lacking, which is seriously restricting the development of multi-channel TPIF microscopy because efficient blue TPIF molecules are absolutely necessary for tagging some specific cellular components. Furthermore, for the probing of some natural molecules, efficient blue emitting molecules are helpful in reducing background light scattering and auto-fluorescence [20–22]. Among the design strategies for TPIF materials, it is pointed out that molecules with short conjugation lengths are expected to possess blue emissions

* Corresponding author. Tel.: +86 21 6425 2756; fax: +86 21 6425 2288.
E-mail address: tianhe@ecust.edu.cn (H. Tian).

0143-7208/$ - see front matter © 2005 Elsevier Ltd. All rights reserved.
doi:10.1016/j.dyepig.2005.11.010

[23,24]. Triphenylamine or diarylamine often used as electron donor and fluorene or benzene can be used as π-conjugated bridge [25–27]. The kind of molecule based on spirosilabifluorene has never been studied as a two-photon absorption material. It is expected that the introduction of spirosilabifluorene in two photon absorption materials will inhibit aggregation of molecules and therefore improve the two-photon absorption cross section [26].

In this work, we report the synthesis of 2,2′-bis(triphenylamine)-9,9′-spiro-9-silabifluorene (spirosila-BF-TPA). The properties such as UV absorption, electrochemical properties, photoluminescence (PL), electroluminescence (EL) and two-photon induced fluorescence imaging of spirosila-BF-TPA were evaluated preliminarily.

2. Experimental section

2.1. Materials

All manipulations involving air-sensitive reagents were performed under an atmosphere of dry argon. Diethyl ether and tetrahydrofuran (THF) were refluxed with sodium and distilled. All other reagents and solvents were used as received from commercial sources unless otherwise stated. The synthesis of 2,2′-dibromo-9,9′-spiro-9-silabifluorene was described in our previous work [28].

2.2. Instrumentation

^{1}H NMR spectra were recorded on a Brucker AM500 spectrometer with tetramethylsilane (TMS) as the internal reference. Mass spectra were obtained on a VG12-250 mass spectrometer. Differential scanning calorimetry (DSC) was performed on a DSC2910 using a heating rate of 10 °C/min and a cooling rate of 10 °C/min. Samples were scanned from 25 to 300 °C and then cooled to 25 °C. UV–vis spectra were measured with Varian Cary 500 spectrophotometer. PL spectra were recorded on a Varian Cary Eclipse spectrophotometer. Cyclic voltammetry (CV) was carried out on a CHI-800 electrochemical workstation with platinum electrodes at a scan rate of 100 mV/s against a Ag/AgCl reference electrode with a solution of 0.1 M tetrabutylammonium perchlorate (Bu_4NClO_4) in acetonitrile (CH_3CN). A femtosecond laser (coherent) with 800 nm pulse (200 fs, 100 MHz) was used as the excitation source and the measurements were performed with a confocal/multi-photon laser scanning microscope (FV300 Olympus); 60× objective (N.A. 1.2) was used to focus the laser beam on samples. A dichromatic mirror RDM650 with a barrier filter BA 480–510 nm was used to decrease the influence of excitation light and luminescence from other fluorophores.

2.3. N,N-Diphenyl-N-(4-bromophenyl)-amine (*8*)

A solution of triphenylamine (5.0 g, 20.4 mmol) in DMF (25 ml) was stirred at room temperature. *N*-Bromosuccinimide (3.6 g, 20.4 mmol) in 25 ml DMF was added in small portions. By addition of NBS, the color of the reaction mixture turned to green. After stirring overnight at room temperature, the reaction mixture was poured into water and was extracted with ether. The organic layer was dried over anhydrous Na_2SO_4. After the solvent was evaporated, the crude greenish oily product was purified by recrystallization from methanol to afford *N*,*N*-diphenyl-*N*-(4-bromophenyl)-amine in 74% yield (4.9 g). ^{1}H NMR (500 MHz; $CDCl_3$): δ (TMS, ppm) 7.35–7.30 (m, 2H), 7.28–7.21 (m, 4H), 7.10–6.98 (m, 6H), 6.95–6.92 (m, 2H).

2.4. N,N-Diphenyl-4-aminophenylboronic acid (*9*)

The Grignard reagent, prepared from *N*,*N*-diphenyl-*N*-(4-bromophenyl)-amine (4.0 g, 12.3 mmol) and 0.4 g (15.0 mmol) magnesium in dry THF (40 ml) was stirred and cooled to −78 °C; a solution of trimethyl borate (2.1 g, 20 mmol) in dry THF (5 ml) was added. After complete addition, the reaction mixture was allowed to slowly come to room temperature. A solution of conc. HCl (2 ml) in ice-cold water (50 ml) was added into the white suspension. The organic phase was separated and washed with brine before drying over anhydrous Na_2SO_4. The solvent was evaporated and the crude product was purified by column chromatography on silica gel with a gradient of dichloromethane/ether to afford *N*,*N*-diphenyl-4-aminophenylboronic acid as a pale yellow solid (1.8 g, 6.2 mmol, 50%). ^{1}H NMR (500 MHz; DMSO-d_6): δ (TMS, ppm) 7.88 (s, 2H), 7.67 (d, 2H, $J = 8.3$ Hz), 7.30 (t, 4H, $J = 7.8$ Hz, 7.7 Hz), 7.10–6.98 (m, 6H), 6.88(d, 2H, $J = 8.3$ Hz).

2.5. 7,7-bis-(N,N-Diphenyl-4-aminophenyl)-9, 9-spirosilabifluorene (*10*, spirosila-BF-TPA)

2,2′-Dibromo-9,9′-spiro-9-silabifluorene (100 mg, 0.204 mmol), 118 mg (2 × 0.204 mmol) triphenylamine boronic acid, and 20 mg of tetrakis(triphenylphosphine)palladium(0), were slurred in a mixture of 14 ml of THF and 7 ml of potassium carbonate solution. The mixture was then refluxed under Ar for 20 h. When the reaction was completed, water was added to quench the reaction. The organic solvent was evaporated and extracted with chloroform. The organic layer was dried over anhydrous $MgSO_4$ and evaporated under vacuum. The crude solid was purified by chromatography on silica gel, using CH_2Cl_2/hexane as the eluent to give spirosila-BF-TPA as white solid (60 mg); m.p. 224–226 °C. ^{1}H NMR (500 MHz; DMSO-d_6): δ (TMS, ppm) 7.80–7.70 (m, 4H), 7.65 (d, 4H), 7.55 (d, 2H), 7.47 (t, 2H), 7.38–7.25 (m, 10H), 7.21(t, 2H), 7.10–7.00 (m, 16H), 6.85 (s, 2H). MS: 818 (100%).

2.6. Fabrication and testing of OLEDs

A two-layer OLED was fabricated by vacuum deposition with a configuration of ITO (30 Ω/square)/(spirosila-BF-TPA) (60 nm)/Alq_3 (80 nm)/Al (100 nm), in which spirosila-BF-TPA was used as a hole injecting and transporting layer, and Alq_3 acts as electron transporting emitter layer. Before loading into a deposition chamber, the ITO substrate

was cleaned with detergents and deionized water, dried in an oven at 120 °C for about 2 h, and treated with UV–ozone for 25 min. The device was fabricated by evaporating organic layers at a rate of 0.1–0.3 nm/s onto the ITO substrate sequentially at a pressure below 5×10^{-6} mbar. Onto the Alq_3 layer a 100-nm thick Al layer was deposited at a rate of 0.6 nm/s as the cathode. For comparison, a single layer Alq_3 (80 nm) device was also prepared and tested under identical conditions. The current–voltage–luminance characteristics were measured with a Spectrascan PR 650 photometer and a computer-controlled DC power supply under ambient conditions.

3. Results and discussion

3.1. Synthesis

The general synthetic routes are shown in Scheme 1. In our previous works, the conversion of dibrominated triphenylamine into triphenylamine diboronic acid was achieved by a two-step synthesis: lithiation arylhalide with an excess of *n*-BuLi, followed by treating it with trimethyl borate [28]. However, we cannot obtain compound **9** by the same method. So compound **9** was prepared by Grignard regent. Compound **10** was prepared from a Suzuki coupling reaction between dibromide **6** and the boronic acid **9**. Compounds **6**, **9**, and **10** were characterized by ^{1}H NMR spectra and mass spectral data.

3.2. Thermal properties

The thermal properties of the spiro-linked triphenylamine derivative were investigated by differential scanning calorimetry (DSC). DSC was performed in the temperature range from 25 to 350 °C. Fig. 1 displays the DSC curves of a sample recrystallized from dichloromethane/hexane. The sample melts at 225 °C on heating, no glass transition phenomenon occurred and no exothermic peak due to crystallization was observed. On subsequent cooling and heating cycles, only the melting peak appears again when the sample is reheated. *N*,*N*′-bis(3-Methylphenyl)-*N*,*N*′-diphenyl-[1,1′-biphenyl]-4,4′-diamine (TPD) and *N*,*N*′-di(1-naphthyl)-*N*,*N*′-diphenyl-[1,1′-biphenyl]-4,4′-diamine (α-NPD) have been widely used as hole transporters in organic EL devices; however, these materials are not thermally stable. TPD is not morphologically stable either, tending to crystallise readily. A number of hole transporting amorphous molecular materials with higher T_gs than those of TPD and α-NPD have been developed on the basis of the guideline of the incorporation of rigid moieties, which include 4,4′,4″-tri(*N*-carbazolyl)triphenylamine [29],

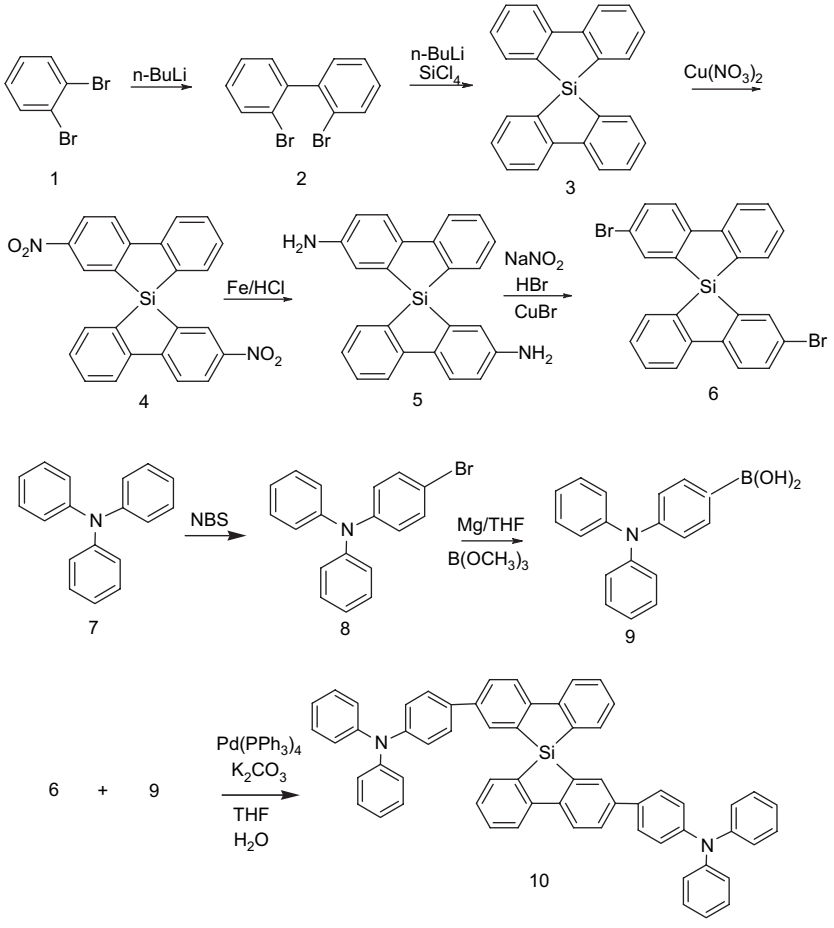

Scheme 1. The synthetic route of spirosila-BF-TPA.

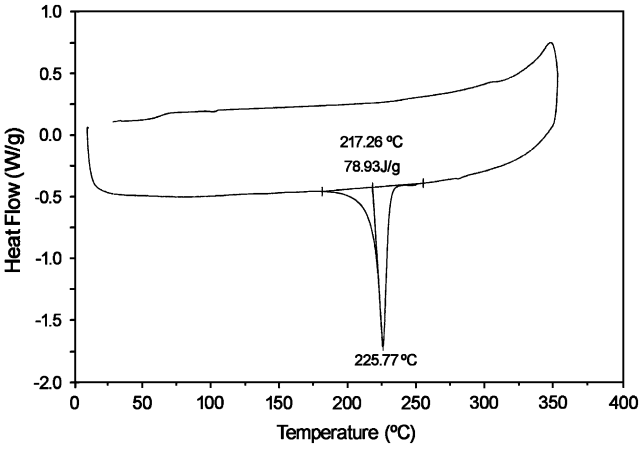

Fig. 1. DSC thermograms of spirosila-BF-TPA.

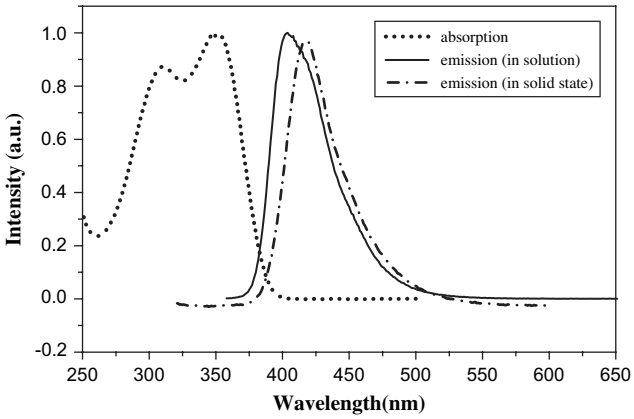

Fig. 2. Absorption and emission spectra of spirosila-TPA.

tri(9,9′-dimethylfluoren-2-yl)amine [30], 2,2′,7,7′-tetrakis-(*N*,*N*-diphenylamino)-9,9′-spirobifluorene [1] and so on. The T_g values of most these materials are below 165 °C. It is evident that the thermal stability of spirosila-BF-TPA is significantly higher than most hole transporting materials. These comparisons illustrate the fact that the incorporation of rigid 9,9′-spiro-9-silabifluorene units into the molecule backbone increases the molecule rigidity and results in a higher thermal stability.

3.3. Electrochemical properties

The electrochemical behavior of spirosila-BF-TPA was investigated by cyclic voltammetry. We could record only p-doping processes and unable to record n-doping processes. Spirosila-BF-TPA showed reversible p-doping processes. In the anodic scan, the oxidation (p-doping) started at about 0.93 V, which is very close to the data reported for triphenylamine $E_{ox} = 0.9$ V and $I_p = 5.3$ eV. So the oxidation is attributed to p-doping of triphenylamine segments. The arylamine donor functionality leads to a significant reduction in oxidation potential. HOMO level was calculated according to an empirical formula, HOMO $= -(E_{ox} + 4.4)$ eV. HOMO of spirosila-BF-TPA was estimated to be −5.33 eV. The high-lying HOMO energy level and reversible electrochemical oxidation of spirosila-BF-TPA suggest that spirosila-BF-TPA has potential to be used as material for hole injection and transport in OLEDs [31]. It is also worth mentioning that the spiro-linked triphenylamine moieties are noninteracting redox centers, as they are electrochemically equivalent and oxidize simultaneously at the same potential [32,33]. This observation is consistent with the notion that the sp^3-hybridized silicon atom at the spiro center effectively interrupts the conjugation.

3.4. Optical properties

Fig. 2 depicts the absorption and photoluminescence (PL) spectra of spirosila-BF-TPA in dilute solution (1×10^{-5} M). Spirosila-BF-TPA shows two absorption maxima at around 311 and 348 nm. Upon excitation, the solution exhibits a vibronic fine-structure with a sharp peak at 406 nm. There is no signature of 9,9′-spiro-9-silabifluorene emission and the triphenylamine emission. In general, the presence of a well-defined vibronic structure in the emission spectrum indicates that the material has a rigid and well-defined backbone structure [34].

In comparison to dilute solution, the emission spectrum of the solid state powder shows 11 nm red-shift. The red-shift of the emission observed in the solid state is probably due to the different relative permittivity of the environment.

3.5. Electroluminescent properties

In this study an EL device was fabricated using spirosila-BF-TPA as a hole injecting and transporting layer, tris(8-hydroxyquinolinato)-aluminum (Alq_3) as the electron transporting emitter layer, ITO as the anode, and Al as the cathode to form a two-layer OLED with a structure of ITO/(spirosila-BF-TPA) (60 nm)/Alq_3 (80 nm)/Al (100 nm) (type 1). To evaluate the hole injecting and transporting ability of spirosila-BF-TPA, a reference OLED with a structure of ITO/Alq_3 (80 nm)/Al (100 nm) (type 2) was simultaneously fabricated under the same vacuum cycle for comparison. Both type 1 and type 2 devices showed pure green EL from Alq_3. Fig. 3 shows the current–voltage–luminance characteristics of the two OLEDs. At a given voltage, the current density of type 1 device is lower than that of type 2 device. The turn-on voltage of type 1 device is lower than that of type 2 device. Type 1 device has a brightness of 400 cd/m^2 at 15 V, while type 2 device has a maximum luminescence of 45 cd/m^2 at 20 V. Fig. 4 illustrates the current efficiency–power efficiency–current density characteristics of the two devices. Type 2 device gives a maximum current efficiency of 0.020 cd/A. The current efficiency of type 1 device shows remarkable enhancement to a maximum value of 0.75 cd/A. The power efficiency of type 1 device can reach 0.22 lm/W, which is 44 times than that (0.0051 m/W) of type 2 device.

The remarkable enhancement in brightness and efficiency of the spirosila-TPA-based device can be attributed to the better balanced charge recombination at the emitting

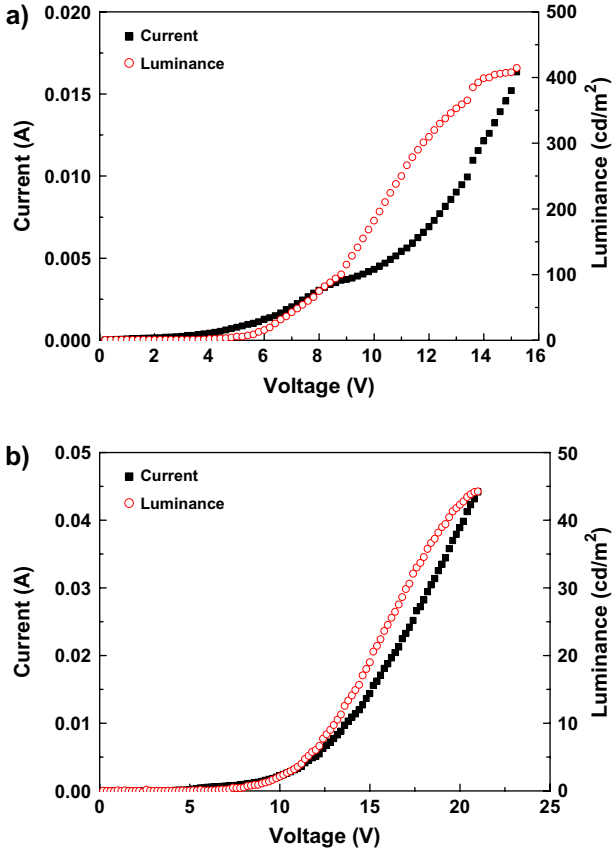

Fig. 3. The current–voltage–luminance characteristics of the two devices: (a) ITO/(spirosila-BF-TPA)/Alq_3/Al and (b) ITO/Alq_3/Al.

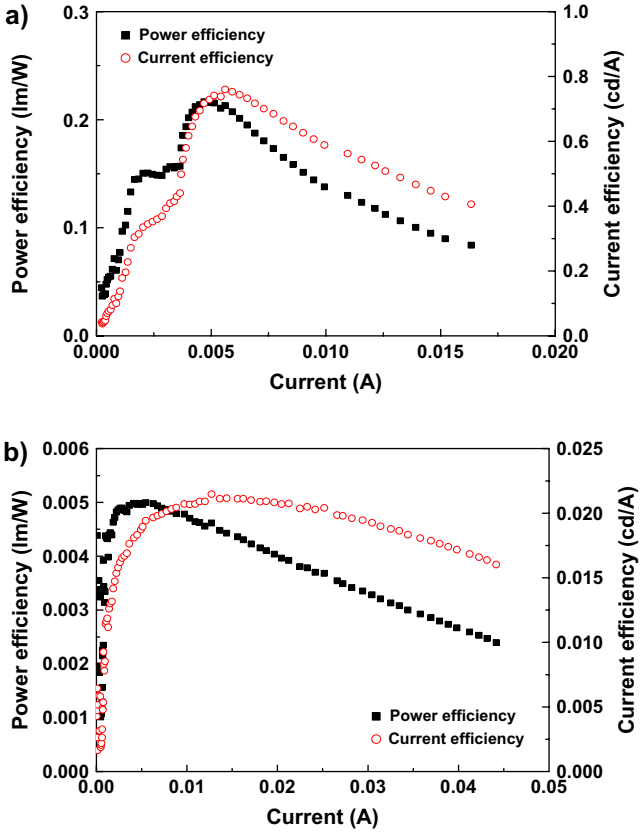

Fig. 4. The current–power efficiency–current density curves of the devices: (a) ITO/(spirosila-BF-TPA)/Alq_3/Al and (b) ITO/Al_3/Al.

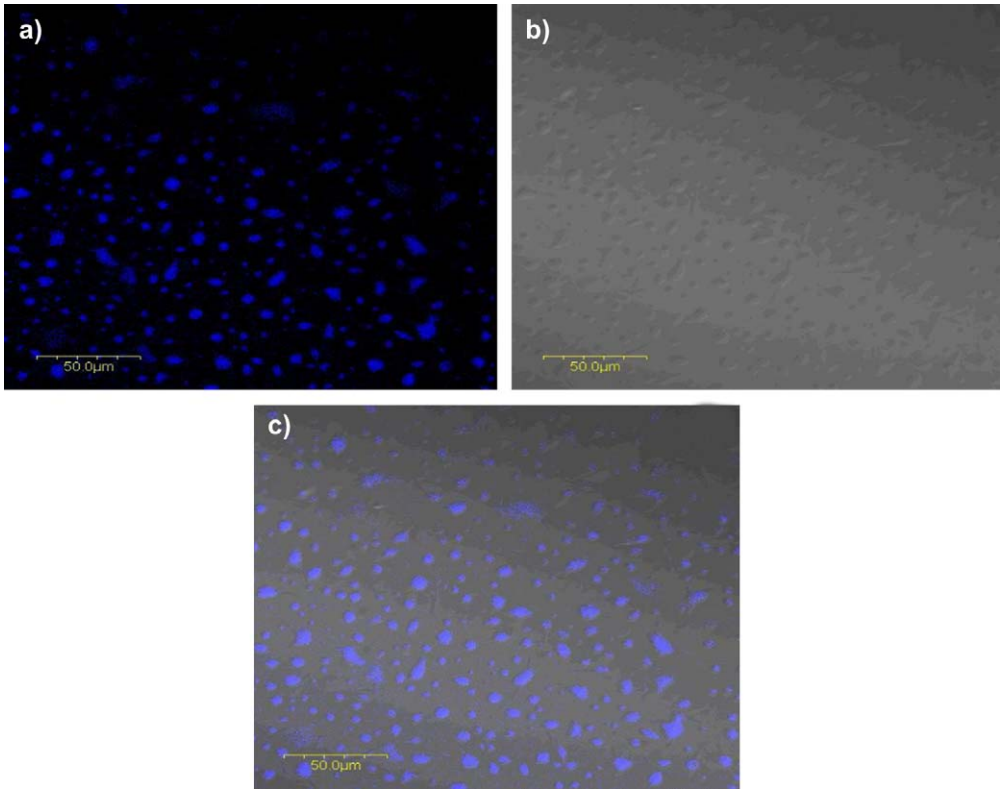

Fig. 5. The two-photon fluorescence images of spirosila-BF-TPA film. (A) The two-photon fluorescent image, (B) the differential interference contrast image, and (C) the merged image of (A) and (B).

interface. It has been shown that the usage of spirosila-BF-TPA with hole transport ability decreases the electron current and thus the amount of electron surplus at the emitting interface. As a result, the hole and electron injected into the emitting layer is better balanced compared to the reference Alq_3 device, and the brightness and efficiency are significantly enhanced. Although the device lifetimes were not tested and compared in the present study, a high stability for the spirosila-BF-TPA-containing device is expected due to the high morphological and thermal stabilities of spirosila-BF-TPA as judged by DSC measurements. The results indicated that spirosila-BF-TPA could function as a hole transporting material used in organic LEDs.

3.6. Confocal/multi-photon microscope of spirosila-BF-TPA films

The films were prepared by drying CH_3CN solutions containing spirosila-BF-TPA on a glass substrate. Fig. 5 shows the two-photon fluorescence images of spirosila-BF-TPA films. Fig. 5A is the two-photon fluorescent image. Fig. 5B is the differential interference contrast image, which was fabricated to verify the fluorescence in Fig. 5A is induced by two-photon absorption of spirosila-BF-TPA. The merged image of A and B is shown in Fig. 5C. According to the results, the two-photon fluorescence of spirosila-BF-TPA is really intensive and further investigation is under progress.

4. Conclusions

In summary, a novel material spirosila-BF-TPA was derived from 2,2′-dibromo-9,9′-spiro-9-silabifluorene and triphenylamine boronic acid was synthesized by palladium(0)-catalyzed Suzuki coupling reaction. Attributed to the spiro structure, spirosila-BF-TPA exhibits a high thermal stability and no glass transition temperature was observed. Spirosila-BF-TPA possesses reversible oxidation process and low ionization potential (5.33 eV). The hole transport ability of spirosila-BF-TPA was verified by comparing the electroluminescent properties of two types OLED devices. According to the fluorescence images of spirosila-BF-TPA films, it was found that the two-photon fluorescence of the sample is intensive. It is expected that this molecule is a promising candidate for applications such as two-photon microscopy and hole transporting material.

Acknowledgements

This project was financially supported by NSFC/China and Education Committee of Shanghai and Scientific Committee of Shanghai. H.T. thanks Prof. J.Y. Chen (Department of Physics, Fudan University, Shanghai/China) for his help in the measurements of the two-photon fluorescent images and Prof. D.G. Ma (Changchun Institute of Applied Chemistry, CAS, Changchun/China) for their measurements of the OLED.

References

[1] Tang CW. Appl Phys Lett 1986;48:183.
[2] Okutsu S, Onikubo T, Tamano M, Enokida T. IEEE Trans Electron Devices 1997;44:1302.
[3] Shirota Y. Organic light-emitting materials and devices. In: Kafafi Z, editor. Proc SPIE, vol. 3148. 1997. p. 186.
[4] Giebeler C, Antoniadis H, Bradley DDC, Shirota Y. Appl Phys Lett 1998;72:2448.
[5] Fujikawa H, Tokito S, Taga Y. Synth Met 1997;91:161.
[6] Tokito S, Tanaka H, Noda K, Okada A, Taga Y. Appl Phys Lett 1997;70:1929.
[7] Konne BE, Loy DE, Thompson ME. Chem Mater 1998;10:2235.
[8] O'Brien DF, Burrows PE, Forrest SR, Konne BE, Loy DE, Thompson ME. Adv Mater 1998;10:1108.
[9] Steuber F, Staudigel J, Stössel M, Simmerer J, Winnacker A, Spreitzer H, et al. Adv Mater 2000;12:130.
[10] Shirota Y. J Mater Chem 2000;10:1.
[11] Salbeck J, Bauer J, Weissörtel F. Macromol Symp 1997;125:121.
[12] Johansson N, Dos Santos DA, Guo S, Cornil J, Fahlman M, Salbeck J, et al. J Chem Phys 1997;107:2542.
[13] Johansson N, Salbeck J, Bauer J, Weissörtel F, Bröms P, Andersson A, et al. Adv Mater 1998;10:1136.
[14] Wu R, Schumm JS, Pearson DL, Tour JM. J Org Chem 1996;61:6906.
[15] Ohshita J, Lee K-H, Hamamoto D, Kunugi Y, Ikadai J, Kwak Y-W, et al. Chem Lett 2004;33:892.
[16] Mitschke U, Bauerle P. J Chem Soc Perkin Trans 1 2001:740.
[17] Denk W, Strickler JH, Webb WW. Science 1990;248:73.
[18] Albota M, Beljonne D, Brédas JL, Ehrlich JE, Fu JY, Heikal AA, et al. Science 1998;281:1653.
[19] Helmchen F, Denk W. Curr Opin Neurol 2002;12:593.
[20] Xu C, Williams RM, Zipfel W, Webb WW. Bioimaging 1996;4:198.
[21] Blab GA, Lommerse PHM, Conget L, Harms GS, Schmidt T. Chem Phys Lett 2001;350:71.
[22] Harms GS, Cognet L, Lommerse PHM, Blab GA, Schmidt T. Biophys J 2001;80:2396.
[23] Valeur B. Molecular fluorescence – principles and applications. Weinhaim, Germany: Wiley-VCH; 2002. p. 48–71.
[24] Huang ZL, Lei H, Li N, Qiu ZR, Wang HZ, Guo JD, et al. J Mater Chem 2003;13:708–11.
[25] Hua J-L, Li B, Meng F-S, Ding F, Qian S-X, Tian H. Polymer 2004;45:7143–9.
[26] Meng F-S, Mi J, Qian S-X, Chen K-C, Tian H. Polymer 2003;44:6851–5.
[27] Reinhardt BA, Brott LL, Clarson SJ, Dillard AG, Bhatt JC, Kannan R, et al. Chem Mater 1998;10:1863–74.
[28] Xiao H-B, Leng B, Tian H. Polymer 2005;46:5707–13.
[29] Kuwabara Y, Ogawa H, Inada H, Noma N, Shirota Y. Adv Mater 1994;6:677.
[30] Shirota Y. J Mater Chem 2005;15:75–93.
[31] Chiang C-L, Shu C-F. Chem Mater 2002;14:682.
[32] Flanagan JB, Margel S, Bard AJ, Anson FA. J Am Chem Soc 1978;100:4248.
[33] Shu CF, Shen HM. J Mater Chem 1997;7:47.
[34] Wu F-I, Dodda R, Reddy DS, Shu C-F. J Mater Chem 2002;12:2893.